

G. Girish Kumar · N. Munichandraiah

Ageing of magnesium/manganese dioxide primary cells

Received: 24 August 1999 / Accepted: 2 December 1999

Abstract Mg/MnO₂ primary cells which were more than a decade old were investigated for their discharge capacity, a.c. impedance behaviour, delay time, effect of added water into the cell and effect of temperature. Although the cells were aged for a long duration, they were electrochemically active and yielded good discharge capacity, thus suggesting an extraordinary long shelf-life. There was a marginal increase in cell capacity subsequent to injection of 2 ml of water into a CD-size Mg/MnO₂ cell. The a.c. impedance of a partially discharged cell included the contributions of surface passive film on the Mg anode and corrosion of the Mg metal. The internal resistance of the cell was found to increase with storage time, suggesting that the resistance of a fresh cell also could similarly increase. By increasing the cell temperature, the impedance decreased considerably and also the delay time. These results suggested that the increase of temperature had favourable effects on the performance of the aged Mg/MnO₂ cells.

Key words Magnesium/manganese dioxide cell · Ageing · Delay time · Temperature effect · A.c. impedance

Introduction

Primary batteries occupy great importance in the consumer market for a wide range of applications, despite intense research efforts that have been carried out for the development and commercialization of high-energy rechargeable systems such as lithium-ion batteries. The conventional Leclanché cell, viz., the zinc/manganese

dioxide cell, and a recent alkaline zinc/manganese dioxide cell are presently in use. The magnesium/manganese dioxide primary cell is not popular either in research laboratories or in the consumer market in spite of the fact that it offers several advantages over the Zn/MnO₂ cell [1]. The difference between the two cell systems is in the electrochemistry of the anode material, while the electrochemistry of the MnO₂ remains unaltered. The standard electrode potential of the Mg anode is -2.37 V against -0.76 V for the Zn anode; the electrochemical specific capacity of Mg is 2.2 Ah g⁻¹ against 0.83 Ah g⁻¹ for Zn and the density of Mg is 1.74 g cm⁻³ against 7.14 g cm⁻³ for Zn. In addition to these favourable electrochemical features for achieving higher energy density for the Mg/MnO₂ cell than the Zn/MnO₂ cell, the resources for Mg are plentiful. Another interesting aspect is that the Mg/MnO₂ cells can be stored for a much longer time (i.e., higher shelf-life) than the Zn/MnO₂ cells. The higher shelf-life is attributed to the presence of a coherent passive oxide film on the Mg anode, which prevents perforations on the Mg anode due to localized corrosion. Recently, Mg/MnO₂ cells, which were more than a decade old and had been stored in an ambient laboratory environment, were investigated for their electrochemical impedance behaviour at different depths of discharge [2]. The internal resistance of an undischarged cell was extremely high (>10 k Ω), but it decreased with an increase of depth of discharge and reached a value as low as 7 Ω at the end of discharge. The extraordinary high shelf-life of the Mg/MnO₂ cell could be attributed to the high resistance of the surface passive film on Mg. However, it is not clearly understood whether a prolonged storing of the cell imparts such a high resistance to the surface film. In order to examine this aspect, in the present studies, partially discharged cells were subjected to a.c. impedance measurements for more than 6 months. Also, the effect of addition of water on the discharge capacity and the effect of temperature on the delay time of the aged Mg/MnO₂ cells were studied.

G. Girish Kumar · N. Munichandraiah (✉)
Department of Inorganic and Physical Chemistry,
Indian Institute of Science,
Bangalore 560 012, India
e-mail: muni@ipc.iisc.ernet.in

Experimental

The Mg/MnO₂ cells of CD size were manufactured by Bharat Electronics, India. Mg-AZ21 alloy, in the form of a can, served both as the anode material and the cell container. The cathode material consisted of MnO₂ powder mixed with acetylene black in an aqueous electrolyte of MgClO₄. The cell construction was similar to that of the conventional Zn/MnO₂ cell. The outer side of the Mg can was partially covered with a thin and transparent polymer film, and the top portion of the cell was covered with a layer of coal tar. These cells were manufactured around 1985 and stored in sealed polythene bags in the laboratory environment at ambient temperature. In the present studies, some of the cells were discharged to a closed circuit voltage of 0.8 V at a constant current of 0.2 A to evaluate their discharge capacities. Into each of a few cells, 2 ml of distilled water was injected and the cells were allowed to stand for 24 h before discharge. Experiments were conducted by introducing a Ag/AgCl, Cl⁻ reference electrode (RE) through a hole made in the Mg can. Agar-agar gel containing a saturated solution of KCl was used as the salt bridge.

A galvanostatic circuit consisting of a regulated d.c. power supply in series with a high resistance and an ammeter was employed for the cell-discharge studies. Electrochemical impedance data of the Mg cells were measured by an electrochemical impedance analyser (EG&G PARC model 6310) and a software program (EG&G PARC model 398), which were driven by an IBM compatible computer. The excitation signal used was 5 mV and the frequency range was from 100 kHz to 5 mHz. The experiments were carried out at 20 ± 1 °C with several cells to ensure reproducibility. Cell voltage-time transients on initiating a discharge current were recorded by using a galvanostat/potentiostat (EG&G PARC model Versastat), which was driven by a computer. For the experiments at higher temperatures, the cell was enclosed in an airtight glass container which was surrounded by an electrical heating tape. The required temperature was maintained within ±1 °C using a temperature controller and a sensor.

Results and discussion

In general, the shelf-life of a primary cell (e.g., Zn/MnO₂) is about a year. Beyond the shelf-life period, the cell may exhibit the following problems: the cell loses its capacity, the anode corrodes, the electrolyte leaks through pores formed on the anode, the cathode mix dries out owing to loss of water, the inter-electrode separator deteriorates, and so on. As a result, the primary cells usually cannot be stored for a long time. Although the Mg/MnO₂ cells were assembled more than 10 years ago, they were free from corrosion, thus possessing an extraordinary long shelf-life [2].

Influence of water on cell discharge

Although the capacity of the Mg/MnO₂ cell is limited by the positive electrode material (i.e., MnO₂), it was intended to examine the variation of individual electrode potentials of the aged cells during discharge. This was because the resistance of the surface film on the Mg anode increased to a high value (10 kΩ) during ageing [2] and the reaction products, viz., Mg(OH)₂ or MgO, usually accumulate as a layer and grow thicker adjacent to the anode during discharge. The discharge voltage

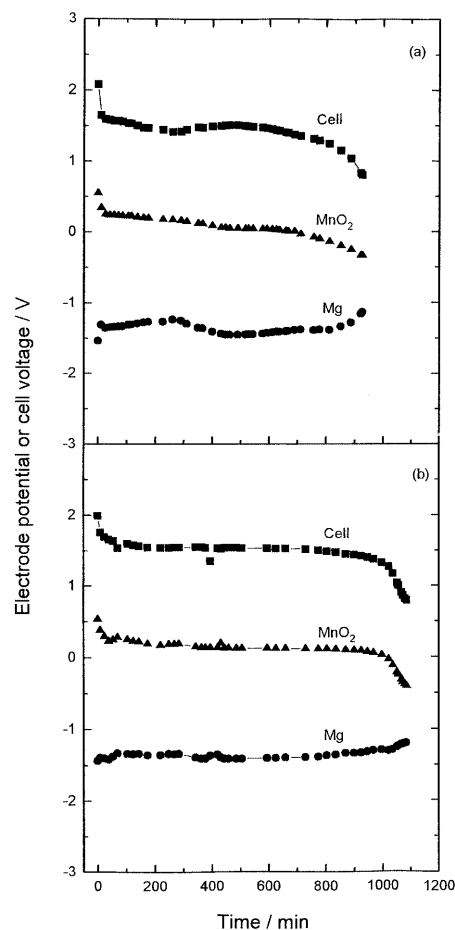


Fig. 1a, b Discharge curves of aged Mg/MnO₂ (CD size) cells and individual electrode potentials at a constant current of 0.2 A at 20 °C. **a** Without water addition and **b** with addition of 2 ml of water. The electrode potentials were measured using a Ag/AgCl, Cl⁻ reference electrode

curve of the aged Mg/MnO₂ cell (Fig. 1a) resembled that of a fresh cell, except for minor fluctuations. Such fluctuations were due to the Mg anode, as reflected by its potential variations during cell discharge. Also, the potentials of both the Mg and the MnO₂ electrodes showed a deflection at the end of discharge, indicating that the cell capacity was limited by both the electrodes.

In order to examine any possible loss of water in the electrolyte during prolonged ageing, 2 ml of distilled water was injected into a Mg/MnO₂ cell and the cell was allowed to stand for about 24 h prior to discharge. The variations of cell voltage and the individual electrode potentials during discharge are shown in Fig. 1b. It was found that the discharge behaviour of the watered cell was free from fluctuations, unlike the case of unwatered cell (Fig. 1a). The cell voltage as well as the individual electrode potential curves were flatter (Fig. 1b). There was a sharp change in the MnO₂ potential at the end of discharge, which corresponded to the sharp decrease in cell voltage. The Mg electrode potential curve was flat throughout the duration of cell discharge. The cell capacity was thus limited by the

positive electrode material in the case of the watered cells. The deflection of the Mg potential of the unwatered cell at the end of discharge (Fig. 1a) might be due to the higher ohmic drop associated with the discharge products of the electrode in a starved condition during continuous discharge. Also, the discharge capacity of the watered cell was higher by about 15% in comparison with the capacity of the unwatered cell. It was thus inferred from these studies that the performance of the aged Mg/MnO₂ cells might be improved marginally by adding water. The a.c. impedance behaviour of unwatered and watered cells were nearly the same, except that the ohmic resistance of the watered cell was slightly less.

Electrochemical impedance spectroscopy

Since the cathode consists of fine particles of porous MnO₂ with a large surface area, the impedance of a Mg/MnO₂ or a Zn/MnO₂ cell was assumed due to the anode and the impedance contribution of the MnO₂ cathode was neglected [3–5]. In order to verify this, the following two types of experiments were carried out. In the first case, a Ag/AgCl, Cl⁻ reference electrode was introduced and the impedances of the cathode and the anode were recorded. The MnO₂ electrode acted as the counter electrode during measurement of the Mg electrode impedance, whereas the Mg electrode acted as the counter electrode during measurement of the MnO₂ electrode impedance. A Ag/AgCl, Cl⁻ reference electrode was present in both the cases. The results are shown in Fig. 2 in Nyquist form. Those for the MnO₂ electrode consisted of a small semicircle at the high-frequency range and a large arc at the low-frequency range (Fig. 2a). The internal resistance of the MnO₂ electrode–Ag/AgCl, Cl⁻ reference electrode combination was less than 1.3 Ω, as obtained by extrapolation of the low-frequency data to the real axis. The resistance, obtained from the diameter of the high-frequency small semicircle, is about 0.1 Ω. Since the Ag/AgCl, Cl⁻ reference electrode reaction is reversible and is expected to have a low impedance value, the high-frequency small semicircle (Fig. 2a) was attributed to the contribution of the reference electrode. Hence, the low-frequency large arc was due to the MnO₂ electrode. On the other hand, the internal resistance of the Mg electrode–Ag/AgCl, Cl⁻ reference electrode combination was about 750 Ω, as obtained from the low-frequency intercept in Fig. 2b. Thus, the magnitude of the impedance of the Mg anode was several times higher than that of the MnO₂ cathode. Furthermore, the magnitude of the impedance of the Mg/MnO₂ cell measured across the positive and negative electrodes was much higher than the individual electrodes' impedance. At any a.c. frequency, the sum of the two electrode impedances was not equal to the cell impedance, similar to the studies on Pb-acid batteries reported in the literature [6]. This was probably due to the fact that the voltage between the concerned electrode and the refer-

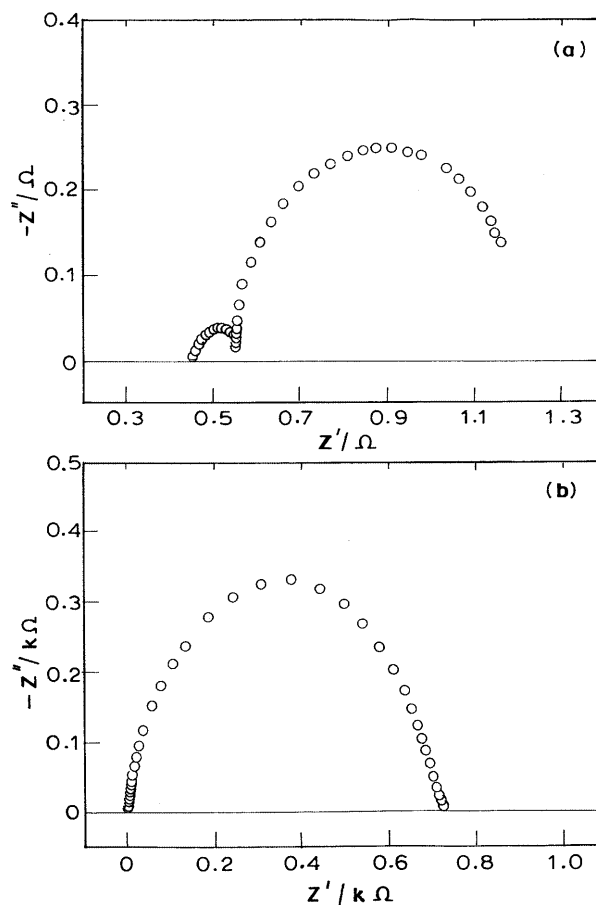


Fig. 2 Nyquist impedance plots of a the MnO₂ cathode and b the Mg anode of a Mg/MnO₂ cell using a Ag/AgCl, Cl⁻ reference electrode

ence electrode, across which the a.c. signal was applied for impedance measurements, was different from the cell voltage.

In the second type of experiments, the bottom portions of Mg cans of two Mg/MnO₂ cells were carefully sectioned out and the two cells were joined together back to back through the cell separator. The combined cell was subjected to impedance measurements between the two Mg anodes and the two MnO₂ cathodes separately. The impedance results are shown in Fig. 3. The impedance results for the two MnO₂ electrodes (Fig. 3a) have taken the shape of two overlapped semicircles with a total resistance of about 9 Ω, which was obtained by extrapolation of the low-frequency data to the real axis. An overlapping of two semicircles suggested a small difference in magnitude of the impedances of the two MnO₂ electrodes. The low-frequency linear spike of the results (Fig. 3a) reflected a diffusion process for the MnO₂ cathode reaction. The impedance of the two Mg electrodes (Fig. 3b) did not take the shape of a semicircle, reflecting capacitive behaviour with an internal resistance of several kilohms. These results also suggested that the impedance of the MnO₂ cathode was negligibly smaller than that of the Mg anode, thus confirming the earlier studies [3–5].

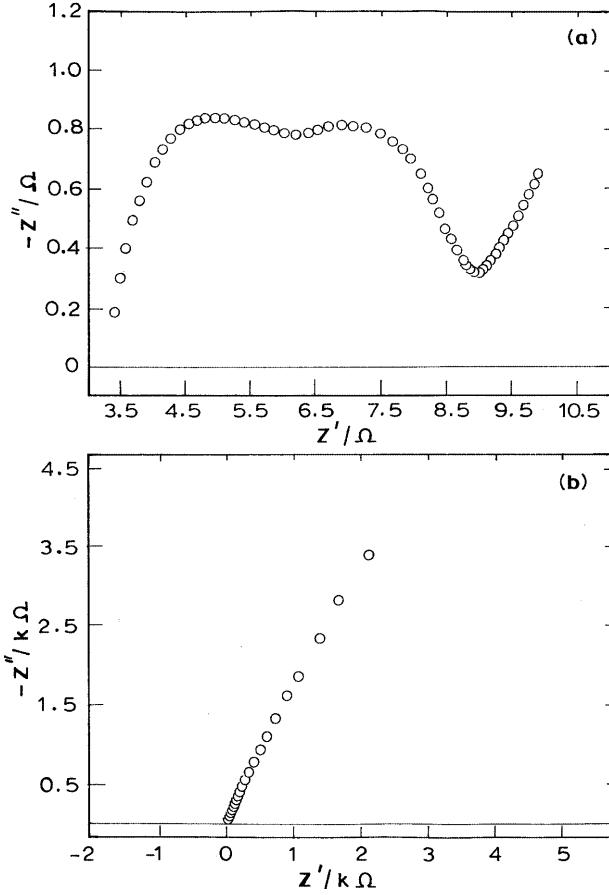


Fig. 3 Nyquist impedance plots of a combined cell **a** between the two MnO_2 cathodes and **b** between the two Mg anodes

It is known that an alkali or alkaline earth metal is covered with a surface film, which constitutes a solid electrolyte interface (SEI) between the metal and the electrolyte [7]. The electron transfer leading to the oxidation of the metal takes place at the metal/surface film interface. At the Mg/electrolyte interface, the surface film on the Mg surface is characterized by its resistance (R_f) and parallel capacitance (C_f). The electron-transfer process at the metal/surface film interface is characterized by charge-transfer resistance (R_{ct}) and a parallel double-layer capacitance (C_{dl}). Additionally, ohmic resistance (R_Ω), which includes the resistances of the cell electrolyte, inter-electrode separator, etc., also contributes to the impedance. The electrical equivalent circuit of the interface comprising these elements is shown in Fig. 4a. The impedance (Z) of the system is, thus given by Eq. 1:

$$Z = R_\Omega + \frac{1/R_f}{(1/R_f^2) + \omega^2 C_f^2} - \frac{j\omega C_f}{(1/R_f^2) + \omega^2 C_f^2} + \frac{1/R_{ct}}{(1/R_{ct}^2) + \omega^2 C_{dl}^2} - \frac{j\omega C_{dl}}{(1/R_{ct}^2) + \omega^2 C_{dl}^2} \quad (1)$$

The Nyquist diagram of the impedance consists of two semicircles, one characteristic of R_f and C_f at the high-

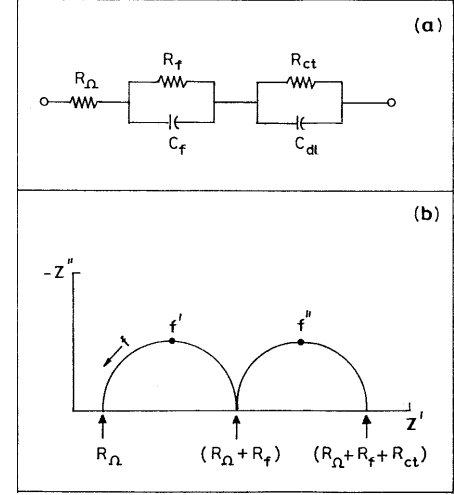


Fig. 4 **a** The equivalent circuit of the Mg anode in a Mg/ MnO_2 cell, and **b** the corresponding schematic complex plane impedance diagram. R_Ω is the ohmic resistance of the cell, R_f and C_f are the resistance and capacitance of the surface passive film on the Mg anode, R_{ct} is the charge-transfer resistance of the Mg corrosion process and C_{dl} is the double-layer capacitance

frequency range and the other characteristic of R_{ct} and C_{dl} at low-frequency range, if the time constants ($R_f C_f$) and ($R_{ct} C_{dl}$) are well separated within the experimental frequency range, as shown schematically in Fig. 4b. The values of R_f and R_{ct} can be obtained from the diameters of the high-frequency and low-frequency semicircles, respectively. The values of C_f and C_{dl} can be calculated using Eqs. 2 and 3:

$$C_f = 1/(2\pi f' R_f) \quad (2)$$

$$C_{dl} = 1/(2\pi f'' R_{ct}) \quad (3)$$

where f' and f'' are frequencies corresponding to the maxima of the semicircles (Fig. 4b). At very low frequencies ($f \rightarrow 0$), Eq. 1 reduces to:

$$Z_{f \rightarrow 0} = R_t = R_\Omega + R_f + R_{ct} \quad (4)$$

where R_t is the internal resistance of the Mg/electrolyte interface and hence the Mg/ MnO_2 cell. At very high frequencies ($f \rightarrow \infty$), the impedance becomes equal to R_Ω :

$$Z_{f \rightarrow \infty} = R_\Omega \quad (5)$$

The interfacial resistance (R_i) of the Mg/electrolyte interface may be defined as:

$$R_i = R_f + R_{ct} \quad (6)$$

If the values of the time constants ($R_f C_f$) and ($R_{ct} C_{dl}$) are close, the two semicircles overlap, resulting in a single semicircle. In such a case, the distinction between R_f and R_{ct} is rather tedious, and therefore R_i and the corresponding interfacial capacitance (C_i) can become useful parameters. The value of C_i can be evaluated from a relationship similar to Eqs. 2 or 3. Although theoretically two clear semicircles are expected, experimentally it was realized only in some cases, as discussed in the

following sections. The criterion for the appearance of two separate semicircles is that the frequencies (f' and f'') corresponding to the maxima of the semicircles should be very different. If these frequencies are not very different, the result is overlapped semicircles. In such a case, it is possible to evaluate the values of R_f , R_{ct} , C_f and C_{dl} by non-linear least squares analysis of the impedance data [8].

Electrochemical impedance of partially discharged Mg/MnO₂ cells

The impedance spectrum of an undischarged and aged Mg/MnO₂ cell did not take the shape of the semicircle or a pair of semicircles, but a linear capacitance spike [2]. The value of the internal resistance thus obtained was about 10 k Ω . The internal resistance decreased to about 140 Ω subsequent to a slight discharge of the cell, and to a value as low as 7 Ω at the end of cell discharge [2]. It is interesting to understand if the surface film resistance increases to about 10 k Ω during the ageing period of about 10 years. Measurement of impedance of the fresh Mg/MnO₂ cells at intervals over a long duration of storing would have provided information on the time dependence of surface film resistance. Alternatively, the Mg anode could be made free from the passive film by subjecting the aged Mg/MnO₂ cell to a partial galvanostatic discharge. It was intended to measure the impedance of the partially discharged cell over a few months of storing. The impedance data of the cell 2 h after discharge to SOC \sim 0.5 are shown in Fig. 5 in Nyquist and Bode plots. The Nyquist plot (Fig. 5a) consists of two capacitive semicircles and an inductive loop at the low-frequency range. Accordingly, the value of the phase angle (ϕ) was negative at the high-frequency range and positive at the low-frequency range (Fig. 5b). The internal resistance (R_i) as obtained from the value of $|Z|$ at low-frequency (Fig. 5b) or from the low-frequency intercept of the Nyquist plot (Fig. 5a) was about 12 Ω .

Impedance behaviour of film-covered metals in passive and transpassive regions of potentials have been of interest [9]. The impedance spectrum of chromium metal in 0.5 M H₂SO₄ in the passive region was almost a vertical line, suggesting that the interfacial impedance was purely capacitive in nature. In the transpassive region, however, the data were seen to fit two semicircles, of which the high-frequency semicircle was capacitive and the low-frequency semicircle was inductive. The inductive behaviour was attributed to the presence of adsorbed intermediates during current flow in the transpassive potential regions. The impedance behaviour of metals in the passive and transpassive regions was theoretically analyzed by invoking a model comprising a metal/metal oxide interface, a metal oxide phase and a metal oxide/solution interface [10]. The total impedance of the system was thus the sum of the impedances of the three components. In order to explain the impedance behaviour, the surface monolayer of the metal oxide was isolated

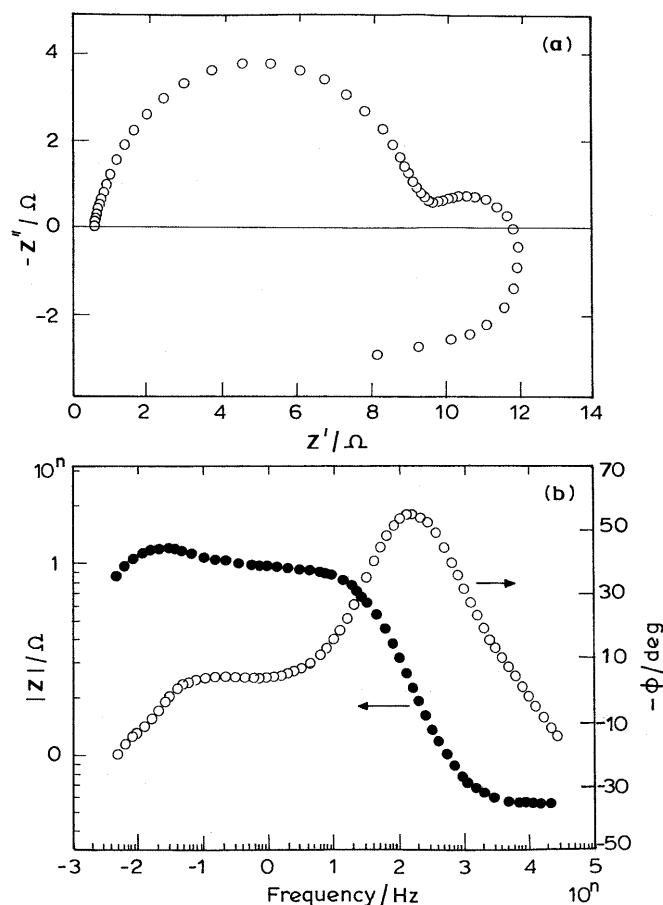
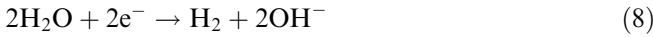
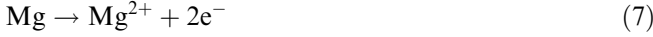


Fig. 5 Electrochemical impedance spectrum in a Nyquist and b Bode forms of an aged Mg/MnO₂ cell 2 h after discharge to SOC \sim 0.5

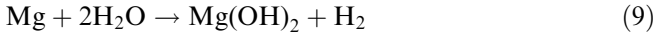
from the rest of the system, and the rates of transfer of metal cations and anions from the bulk of the metal oxide phase as well as from the solutions were taken into consideration. It was shown that when a parameter k ($= 1/\tau$, τ being the relaxation time) was large, the impedance spectrum showed the form of a semicircle. On the other hand, if k was small, two semicircles (either both the semicircles as capacitive, or the high-frequency semicircle as capacitive and the low-frequency one as inductive) were expected in the impedance spectrum during flow of current in the transpassive region. Unlike these studies, which were concerned with impedance behaviour of film-covered metals at different potential regions, the impedance spectrum (Fig. 5) of the partially discharged (SOC \sim 0.5) Mg/MnO₂ cell was recorded at the open-circuit condition.

Since the Mg/MnO₂ cell was partially discharged, the anodic reaction products [viz., Mg(OH)₂ or MgO] accumulated adjacent to the Mg metal. Since the cell was subjected to a continuous discharge to SOC \sim 0.5, the surface of the Mg metal became rough owing to formation of shallow pores during the anodic dissolution of Mg, which could have taken place due to breakdown and simultaneous reformation of a surface passive film. As a result, the metal is less protected by the surface film

and therefore is susceptible to corrosion according to the following reactions:



The above partial reactions of the corrosion process result in an overall reaction:



As described previously, the high-frequency capacitive semicircle was due to a parallel combination of surface film resistance (R_f) and its capacitance (C_f) and the low-frequency capacitive semicircle due to a parallel combination of charge-transfer resistance (or, more specifically, corrosion resistance, R_{ct}) and double-layer capacitance (C_{dl}). The inductive loop might be attributed to the adsorption of H atoms involved in the corrosion reaction (Eq. 8).

The impedance data of the Mg/MnO₂ cells at SOC~0.5 were measured at several intervals during about 6 months of storage. Nyquist plots of some of the results for a cell are shown in Fig. 6. It is seen that the semicircles increased in size during the measurements period. Furthermore, the shape of the plots also changed gradually. The two capacitive semicircles, which were nearly undistorted during the initial periods, merged together resulting in a single distorted semicircle. The size of the single semicircle continuously increased on further storing. The inductive loop was present at all stages of storing.

A continuous increase of the size of the impedance spectrum, and therefore the internal resistance of the

partially discharged Mg/MnO₂ cell over about 6 months, suggested that the internal resistance of a fresh cell could similarly increase during about 10 years of ageing. The impedance parameters, viz., R_f , C_f , R_{ct} , C_{dl} , R_Ω , R_i , C_i , and R_t were plotted as functions of storage time after discharging the cell to SOC~0.5 and are shown in Fig. 7. The parameters R_f , R_{ct} , C_f and C_{dl} were plotted for that duration of storage where the high- and low-frequency capacitive semicircles were clearly separated (Fig. 7a–d). However, the rest of the parameters were plotted encompassing the entire duration of the impedance measurements (Fig. 7e–h). The parameters R_f and R_{ct} increased with time, suggesting an increase in the thickness of the surface film and a simultaneous decrease in the corrosion rate of the Mg metal (Fig. 7a and c). The film capacitance (C_f) is nearly invariant, whereas the double-layer capacitance (C_{dl}) decreased (Fig. 7b and d). Ohmic resistance (R_Ω) showed a gradual increase from about 0.6 Ω to 1.2 Ω in about 6 months storing of the partially discharged cell (Fig. 7e). This might be due to a decrease in the conductivity of the cell electrolyte as loss of water was possible in the corrosion process (reaction 8). The parameters R_i and R_t increased throughout the period of cell storage, whereas C_i decreased to a minor extent. Usually, the interfacial resistance of a film-covered metal is expected to remain invariant after the metal surface is covered with a monolayer of pore-free film. It appears to be rather unusual in the present case that formation and growth of the surface film, which is expected to impart passivity to the Mg metal, continued even 6 months after the Mg/MnO₂ cell was partially discharged. Several possibilities could be considered for the increase in film-resistance:

Fig. 6a–d Nyquist impedance plots of a Mg/MnO₂ cell during ageing subsequent to discharge to SOC~0.5. The number on each curve is the ageing time in days

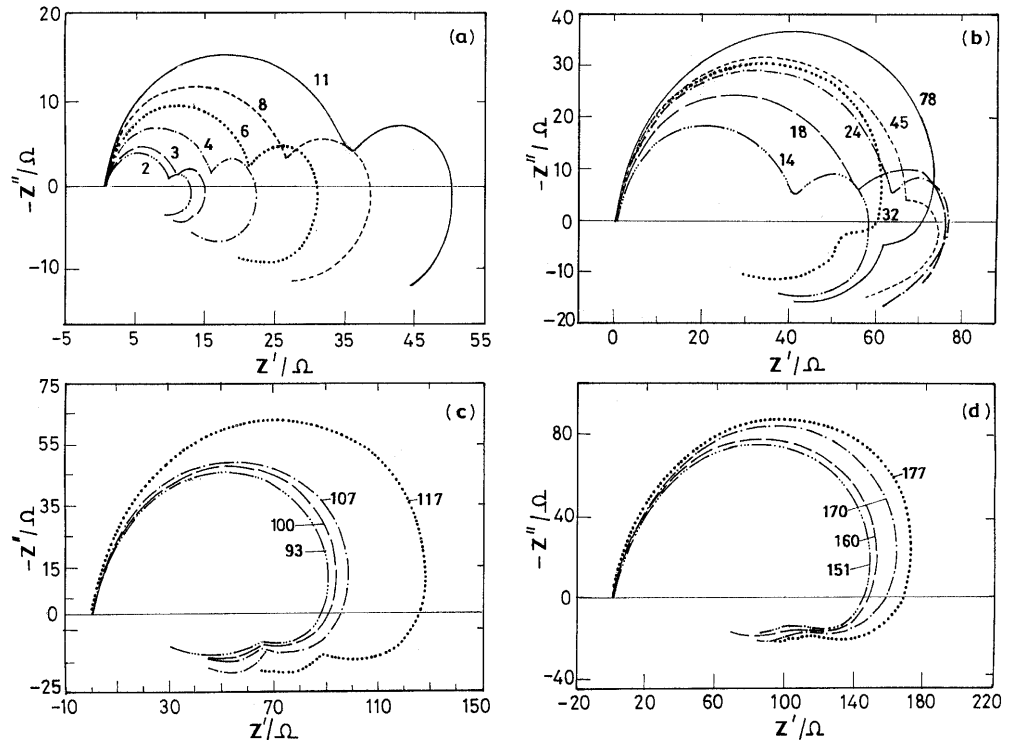
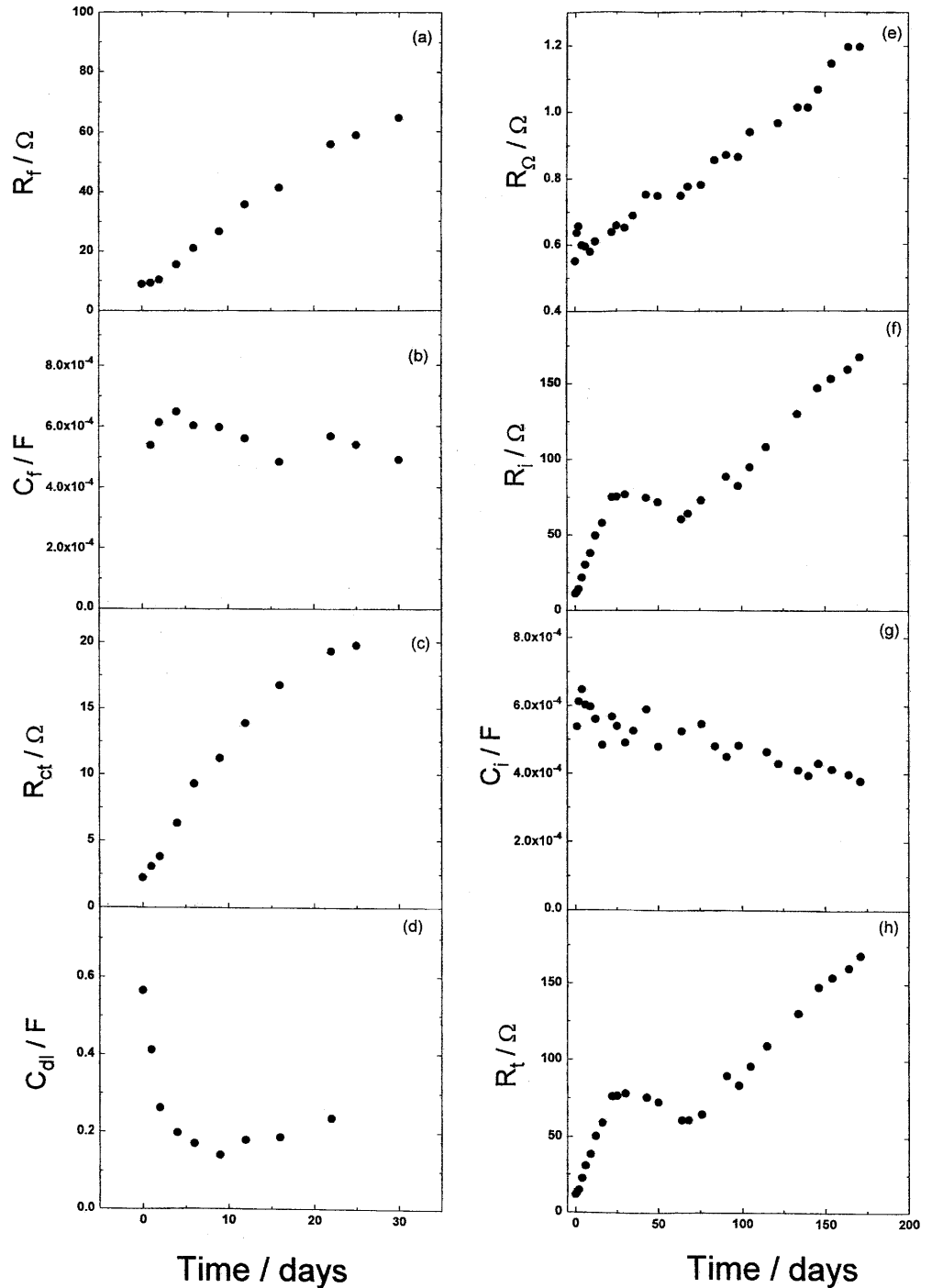


Fig. 7 The impedance parameters **a** surface film resistance (R_f), **b** surface film capacitance (C_f), **c** charge-transfer resistance of corrosion processes (R_{ct}), **d** double-layer capacitance (C_{dl}), **e** ohmic resistance (R_Ω), **f** interfacial resistance (R_i), **g** interfacial capacitance (C_i) and **h** total internal resistance (R_t) of a Mg/MnO₂ cell as a function of ageing time subsequent to discharge to SOC~0.5



1. Owing to the continuous corrosion process through a porous surface film, the thickness of the film and hence its resistance might be increasing.
2. The increase in resistance might be due to the surface film becoming anhydrous owing to its unhygroscopic nature, whereas Mg(ClO₄)₂ in the electrolyte was hygroscopic.
3. The layers of the anodic discharge product adjacent to the Mg metal was also anhydrous and might be becoming a part of the passive film, thus contributing to the increase in surface-film thickness.

4. The MgO or Mg(OH)₂ constituting the surface film of the Mg might be getting converted into a different phase of higher resistivity.

Influence of temperature on impedance of Mg/MnO₂ cells

The influence of temperature on the impedance of the aged Mg/MnO₂ cells of both undischarged (SOC~1) and partially discharged (SOC~0.5) cells was examined.

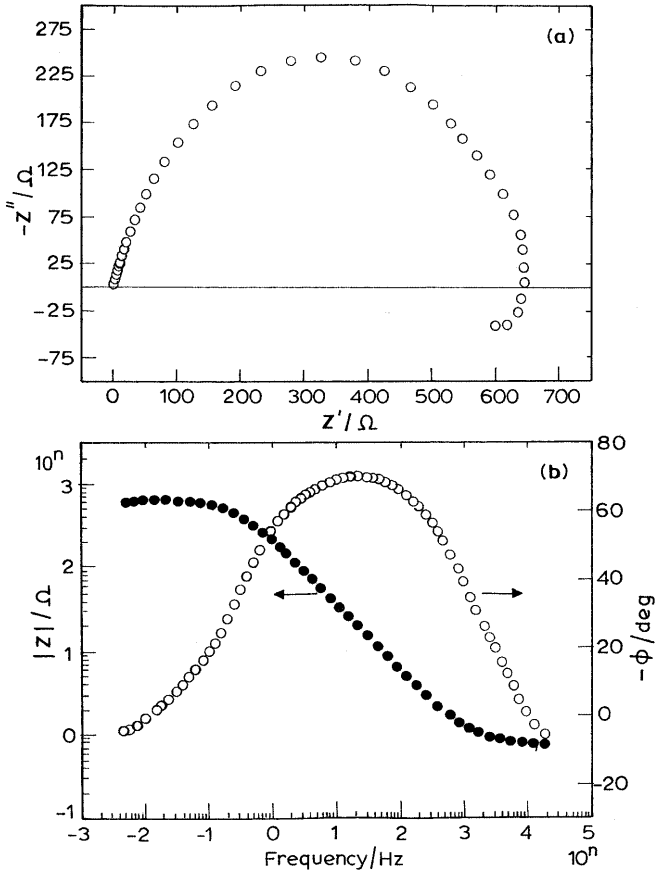


Fig. 8 Electrochemical impedance spectrum of an aged Mg/MnO₂ cell in **a** Nyquist **b** Bode forms at 85 °C

The impedance spectrum of the cell at SOC~1 at 85 °C is shown in Fig. 8. The results have taken the shape of a semicircle in the Nyquist plot (Fig. 8a). The internal resistance of the cell, as measured from the high-frequency intercept of Fig. 8a or by extrapolation of the modulus of impedance ($|Z|$) to abscissa of Fig. 8b, is about 600 Ω . However, the impedance spectrum of the cell at SOC~1 at 20 °C [2] was not in the form of a semicircle in the Nyquist plot and the internal resistance obtained was about 10 k Ω . Thus, a comparison of the data at 20 °C [2] and at 85 °C (Fig. 8) suggested that at higher temperature the impedance of the cell decreased considerably. The decrease in R_i at the higher temperature was due to higher rates of corrosion reaction (reaction 10) and also due to a decrease in R_f of the surface film on Mg, which was ionically conducting. The inverse of the interfacial resistance ($1/R_i$) was found to follow Arrhenius behaviour with temperature and an activation energy of 0.52 eV was obtained (Fig. 9).

Some partially discharged (SOC~0.5) cells were subjected to temperature-dependent impedance measurements at different intervals of storing after discharge. In order to avoid the influence of heating on measurements if the same cell was repeatedly used at different intervals, measurements were conducted using a separate cell at each interval of storage. Nearly at all

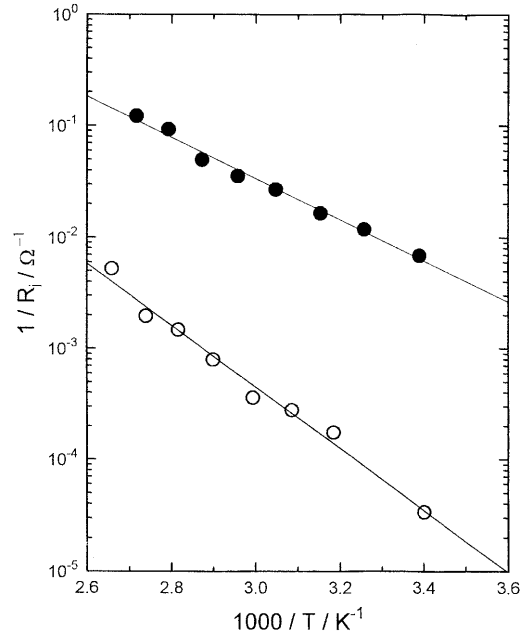


Fig. 9 Arrhenius plot of inverse of interfacial impedance ($1/R_i$) of an aged Mg/MnO₂ cell (○) and a Mg/MnO₂ cell aged for 37 days subsequent to discharge to SOC~0.5 (●)

intervals and temperatures, the impedance spectra were characterized by semicircles, but with varying magnitudes of impedances. The inverse interfacial resistance was found to follow Arrhenius behaviour at all intervals of storage of the partially discharged Mg/MnO₂ cells (Fig. 9). The values of the corresponding activation energies were similar in magnitude with an average value of 0.35 ± 0.02 eV obtained at six different intervals. This result thus suggested that the mechanism of ionic conduction in the surface film and the nature of corrosion process remained nearly the same, although there was an increase in surface film thickness with storage time. The activation energy (0.52 eV) obtained from the aged and undischarged cell was, however, higher than that obtained from the discharged cells (0.35 eV).

Influence of temperature on delay time of the aged Mg/MnO₂ cells

Since the Mg anode is covered by a passive film, breakdown of the surface passive film is a prerequisite for oxidation of Mg to take place during discharge of the Mg/MnO₂ cells [11]. Subsequent to initiation of a galvanostatic discharge, the voltage of the Mg/MnO₂ cell dips to a low value before reaching the normal closed circuit voltage. Consequently, there is a time lag, known as the delay time, during the cell discharge. The voltage-time transients of the aged Mg/MnO₂ cells recorded on initiation of 0.2 A of discharge current at several temperatures are shown in Fig. 10. Each trace was recorded using a separate cell. Open circuit voltage of the cell, closed circuit voltage, voltage dip and delay time on

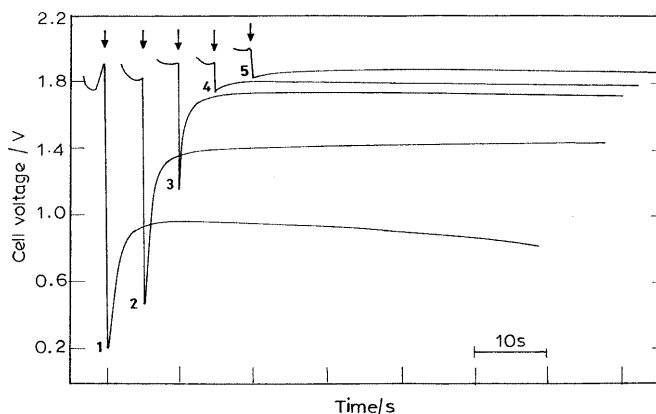


Fig. 10 Voltage-time transients recorded on initiation of 0.2 A of discharge current through aged Mg/MnO₂ cells at 20 (1), 30 (2), 52 (3), 67 (4) and 88 °C (5). An arrow at the top of each curve indicates the moment of initiation of cell discharge

commencement of discharge are plotted against temperature in Fig. 11. On increasing the temperature, the cell voltage increased, the voltage dip before reaching a steady discharge voltage decreased and also the delay time decreased. The increase in cell voltage was attributed to temperature coefficients of individual electrode potentials and also to higher conductivity of the surface film on the Mg metal. The surface film could also be considered to have undergone thermal breakdown, so that exposure of a larger area of film-free Mg metal caused its electrode potential to be more negative. The thermal breakdown of the surface film also accounted for decreased voltage dip and delay time. In fact, the voltage-time transient at 85 °C (Fig. 10, curve 5) suggested negligible voltage dip and delay time. That means that the steady-state discharge voltage is attained almost instantaneously, reflecting negligible influence of the surface passive film on cell discharge.

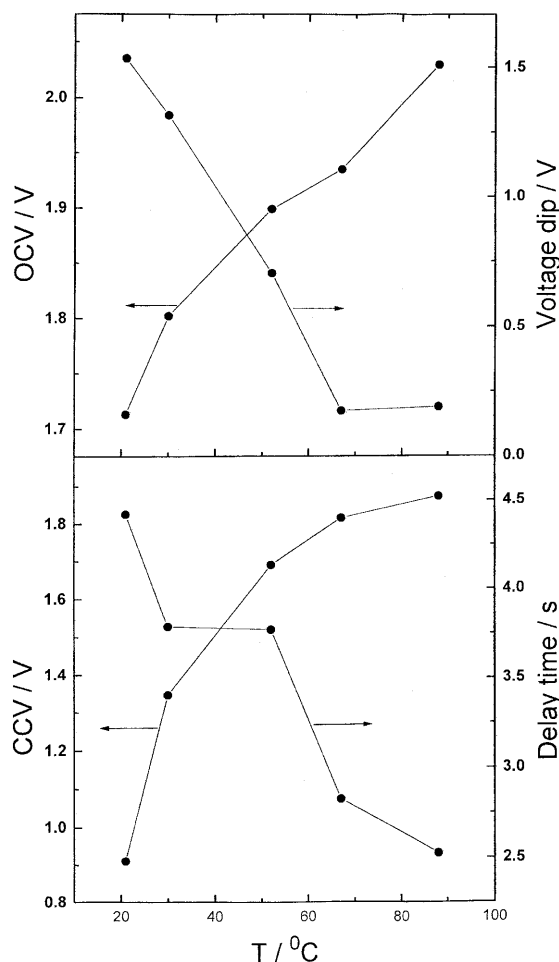


Fig. 11 Variation of open circuit voltage (OCV), closed circuit voltage (CCV), voltage dip and delay time with temperature on initiation of 0.2 A of discharge current through the Mg/MnO₂ cells

Conclusions

The Mg/MnO₂ cells, which were aged more than a decade, were shown to yield good discharge capacity. The capacity increased to some extent on addition of water into the cell. The a.c. impedance of a partially discharged cell reflected the properties of a surface passive film on the Mg as well as the corrosion process. On storing the partially discharged cell, the internal resistance was found to increase during about 6 months, thus suggesting a continuous growth of surface film on Mg during the period of long ageing. Increase of temperature was found to have favourable effect on the cell impedance and also the delay time.

References

1. Robinson JL (1976) Magnesium cells. In: Cahoon NC, Heise GW (eds) The primary battery. Wiley, New York, p 149
2. Munichandraiah N (1999) J Appl Electrochem 29: 463
3. Gopikanth ML, Satyanarayana S (1979) J Appl Electrochem 9: 581
4. Karunathilaka SAGR, Hampson NA, Leek R, Sinclair JJ (1981) J Appl Electrochem 11: 365
5. Root MJ (1985) J Appl Electrochem 22: 1057
6. Keddam M, Stoynov Z, Takenouti H (1997) J Appl Electrochem 7: 539
7. Peled E (1983) Lithium stability and film formation in organic and inorganic electrolytes for lithium battery systems. In: Gabano JP (ed) Lithium batteries. Academic Press, London, p 43
8. Macdonald JR (1987) Data analysis. In: Macdonald JR (ed) Impedance spectroscopy. Wiley, New York, p 173
9. Armstrong RD, Henderson M (1972) J Electroanal Chem 40: 121
10. Armstrong RD, Edmundson K (1973) Electrochim Acta 18: 937
11. Linden D (1995) Handbook of batteries. McGraw-Hill, New York, p 9-1